Chapter

Imaging and AI Techniques in Intrapulmonary Tuberculosis Diagnosis and Management

Victor Chigbundu Nwaiwu

Abstract

Pulmonary tuberculosis (PTB) remains a major health threat worldwide, resulting in millions of deaths yearly, despite ongoing global, regional, and national efforts to eradicate and control this highly infectious disease. The lungs are the primary organs affected, which can be permanently damaged or spread to other body parts if not treated early, medical imaging crucial in diagnosis, assessment, staging, monitoring, and guidance. Chest X-ray (CXR) is the standard initial screening tool for suspected PTB , providing an overall view of structures within the chest. Computed tomography (CT) provides more insights into lymphadenopathy and early bronchogenic spread. Positron emission tomography–computed tomography (PET/CT) is being explored for determining treatment response. Radiological appearances of PTB alongside details from diverse research across these imaging modalities were evaluated. A targeted screening approach involving taking X-ray services down to the doorstep of many in TB-endemic countries, including strategies such as campaigning, mass screening, active case finding, and contact tracing, certainly yielded better results. AI introduction in imaging has surprisingly been instrumental to the recent success and giant strides made in addressing PTB. Empirical studies have demonstrated the remarkable performance of AI techniques such as machine learning (ML), deep learning (DL), natural language processing (NLP), expert systems (ES), robotics, and fuzzy logic (FL) in PTB imaging tasks – worklist management, triaging/prioritization, dose optimization, diagnosis/reporting, and treatment outcome prediction. However, while it is necessary for models to undergo robust training and validation, it is imperative to address growing ethical and regulatory concerns regarding responsible AI use.

Keywords: medical imaging, AI techniques, intrapulmonary tuberculosis, diagnosis, management

1. Introduction

Pulmonary tuberculosis (PTB) is a form of tuberculosis (TB) that affects the lungs, accounting for a large majority (85–90%) of reported TB cases worldwide.

It is the most frequent clinical manifestation of the disease and poses a globally significant health issue, with incidence rates varying significantly by region, from low rates in high-income countries to high rates in low- and middle-income countries, primarily in Asia (45%), Africa (23%), Western Pacific (18%), Eastern Mediterranean (8.1%), Americas (2.9%), and Europe (2.2%) [1, 2].

The prevalence of intrapulmonary TB in 2017 globally was 9.6 cases per 100,000 people, and this figure is projected to increase to 11.4 by 2030. In 2021, statistics reveal that 10.6 million people were affected, with a whopping 6.4 million newly diagnosed TB cases, of which 5.3 million are PTB [2, 3]. Recent figures from the World Health Organization (WHO) reveal a staggering 1.25 million deaths, making it currently the world's leading cause of death from a single infectious agent [4]. Several driving factors are responsible for these abysmal results. The fact that millions of people with intrapulmonary TB are missed by diagnostic systems each year is one factor. Multidrug-resistant TB (MDR-TB), a public health crisis characterized by resistance to at least two of the most effective first-line anti-TB drugs (isoniazid and rifampicin), is yet another factor (estimated 450,000 new cases annually), making standard TB treatments ineffective and resulting in longer, more complex, and expensive treatment courses (nearly 20 times greater than those associated with drug-sensitive TB). Also, the impact of HIV coinfection with TB has worsened treatment outcomes [5]. Despite global efforts that have resulted in saving about 79 million lives since 2000, its easy spread nature and late detection mean the world is unlikely to meet the WHO milestone of a 75% reduction in TB mortality between 2015 and 2025, reports the World Bank [6]. Early detection of intrapulmonary TB remains key to preventing transmission and improving health outcomes [7].

The following medical imaging techniques are proven modalities used to diagnose and manage intrapulmonary TB:

- *Chest radiography (*chest X-ray *[CXR])*
- *Computed tomography (CT)*
- *Positron emission tomography–computed tomography (PET/CT)*

Chest radiography, otherwise called CXR, remains the first-line imaging due to its ready availability, cost-effectiveness, and relatively low radiation dose [8]. Chest X-ray screening services have been very useful in intrapulmonary TB programs in TB-endemic countries (mostly rural areas) faced with a higher burden and greater barriers to accessing health services, which can affect outcomes. Computed tomography is usually resorted to in the detection and characterization of subtle lung lesions, lymphadenopathy, and bronchiectasis [9]. Positron emission tomography–computed tomography (PET/CT) is a hybrid technology that combines the anatomical information from CT with the metabolic information from PET, allowing for the visualization of metabolically active areas and distinguishing between active and inactive TB lesions [10].

The advent of artificial intelligence (AI), rooted in advanced algorithms and learning systems, and its integration with imaging modalities, is beginning to make waves in contemporary TB practice and research in a bid to further improve

intrapulmonary TB diagnosis and management strategies, cutting across aspects of worklist management, prioritization, dose reduction, image quality, and reporting tasks [11]. It is in these imaging and AI directions that this chapter looks to synthesize evidence.

2. Intrapulmonary TB

Intrapulmonary TB is an airborne infectious disease confined in the lungs and caused by the bacteria *Mycobacterium tuberculosis.* The International Consensus for Early TB (ICE-TB) framework distinguishes latent-active paradigm of TB, from disease to infection state that is symptomatic (chest pain, cough, weakness or fatigue, weight loss, night sweats, and loss of appetite) and highly contagious [12].

Latent intrapulmonary TB is commonly diagnosed using a TB skin test (Mantoux test) or a TB blood test (interferon gamma release assay [IGRA]), as imaging tests alone cannot accurately diagnose the latent TB state but help identify individuals at higher risk of progressing from latent to active [13]. Without treatment, latent intrapulmonary TB can develop into active intrapulmonary TB, although it is important to note that not all active cases begin as latent (see **Figure 1**). While some people infected with intrapulmonary TB develop a latent infection (one in four people globally are estimated to have a latent TB infection), it is possible for the infection to progress directly to active disease within weeks or months (see **Figure 2**). Its easy-to-spread nature when in the active state (via airborne droplets released when an infected person coughs or sneezes) makes it quite difficult and challenging to control, which is the reason imaging techniques are crucial for early diagnosis and effective management [14, 15]. Risk factors include exposure to infected persons, congregate settings (homeless shelters, correctional facilities),

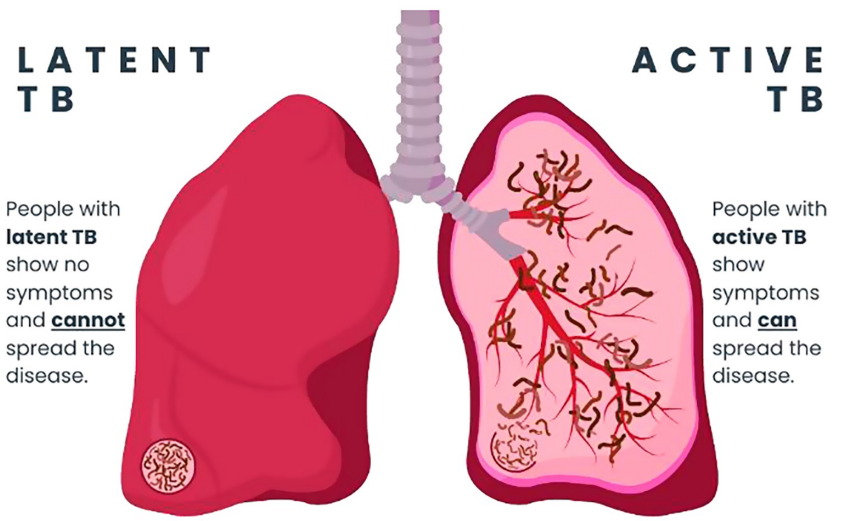

Figure 1.
Latent and active intrapulmonary tuberculosis.

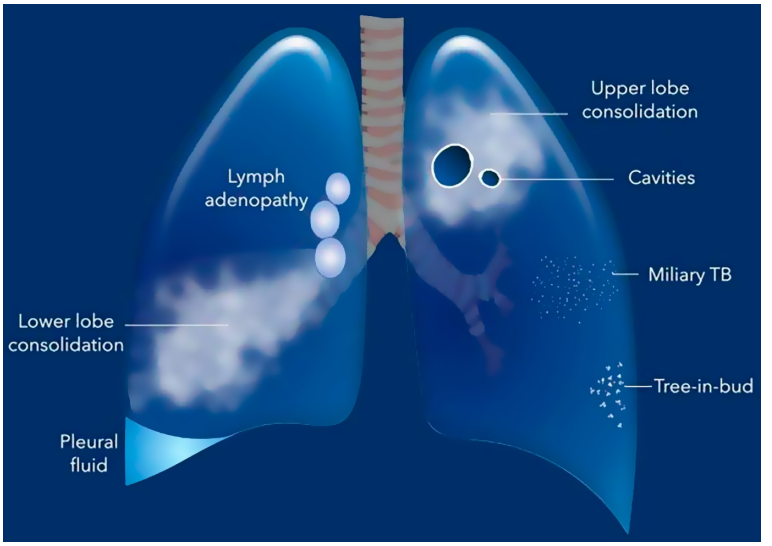

Figure 2.
Active intrapulmonary tuberculosis.

certain health conditions (e.g., diabetes, cancer, kidney disease), environment (being born in or frequently traveling to high TB burden countries), and lifestyle factors (malnutrition, smoking/tobacco use, excessive alcohol consumption) [16, 17]. Following recent studies [18], it has become imperative to disrupt the chain of transmission that sustains the TB epidemic by intensifying efforts in detecting and treating PTB, employing population-wide imaging approaches such as mass screening, targeted chest screening, contact tracing, and further imaging tests [19, 20].

3. Anatomy of the lung

The lungs are large, air-filled, spongy organs, both encased by membranes called the pleura, contained within and protected by the thoracic cage, also known as the rib cage (see **Figure 3**). The right and left main bronchi, which are a continuation of the trachea, alongside blood vessels, nerves, and lymphatic vessels, penetrate and enter each lung on the medial surface in a region called the hilum and thereafter branch extensively throughout the lung. Each lung (right and left lung) is divided anatomically into distinct lobes by fissures, with each lobe containing a portion of the bronchial tree leading into the alveoli [21].

The right lung (slightly shorter and wider than the left) has three lobes: superior, middle, and inferior, and two fissures: horizontal fissure and oblique fissure (the horizontal fissure separates the superior and middle lobes, while the oblique fissure separates the middle and inferior lobes). The left lung has two lobes: superior and inferior, and one fissure: oblique fissure (the oblique fissure separates the superior and inferior lobes) [22].

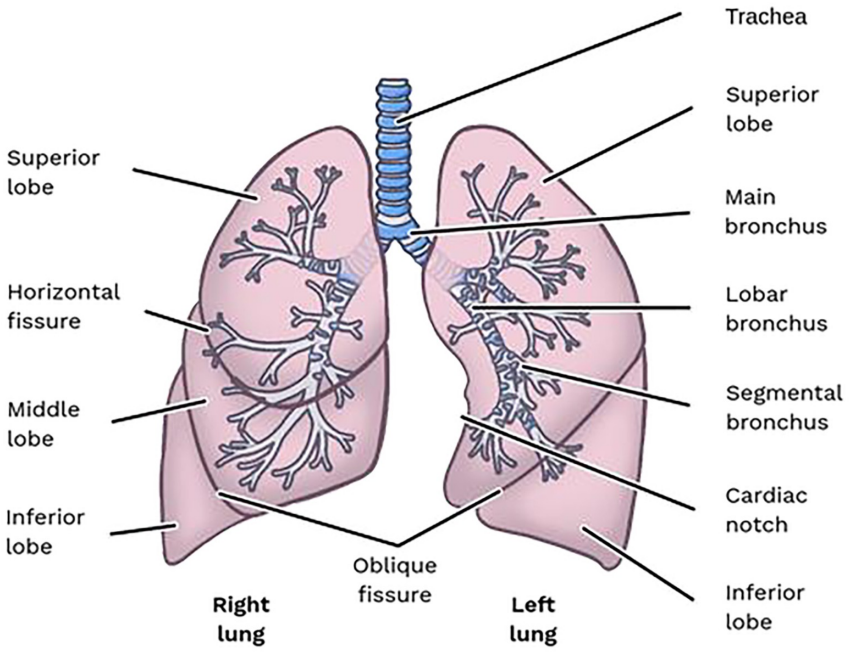

Figure 3.
Anatomy of the lungs.

4. Imaging of intrapulmonary TB (modalities, diagnosis, and assessment)

4.1 Chest X-ray

Conventional chest X-ray is the initial modality employed for screening and diagnosis and remains the standard for detecting and monitoring intrapulmonary TB. It makes use of a small dose of ionizing radiation (approximately 0.1mSv) to produce pictures of the internal structures of the thoracic region (lungs, ribs, heart, airways, blood vessels, bones, and diaphragm), capturing the resulting image on an image receptor system. The image produced depicts different levels of absorption that occur in the various tissues, creating contrast. A standard posteroanterior (PA) and lateral view is the typical initial screening projection, although an anteroposterior (AP) lordotic view may be used as a supplementary projection to better visualize lung apices if obscured [8].

X-ray systems are large, stationary units typically found in hospitals. Nonetheless, due to the need to bring diagnostic services directly to hard-to-reach communities, mobile vans equipped with digital X-ray machines gained traction for rapid and efficient on-site intrapulmonary TB screening to identify and manage cases. The mobile van facility comprises an inbuilt X-ray room, battery/capacitor-assisted X-ray unit and generator, operator/computer room, uninterrupted power supplies (UPS), and lead protective walls/shields (see **Figure 4a**). The use of mobile vans in mass screening campaigns was successful in detecting a large pool of prevalent intrapulmonary TB cases among hard-to-reach populations, and surveys of

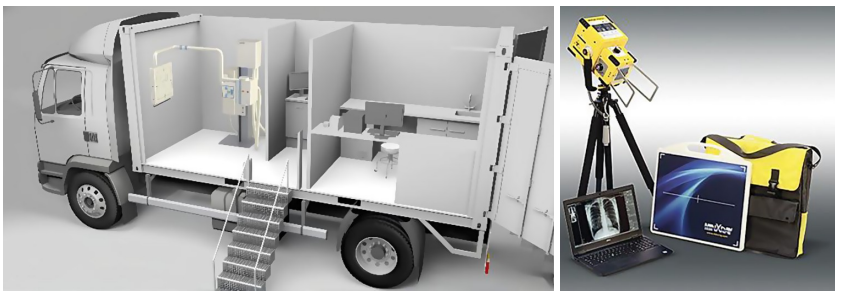

Figure 4.
(a) Mobile van housing compact digital X-ray machine and (b) portable X-ray system.

follow-up campaigns showed significant reductions in the burden of this disease, overcoming socioeconomic barriers and improving access to high-quality TB treatment [23]. A similar mobile van equipped with a digital X-ray machine was again useful in detecting 236 (3.4%) TB cases out of 6,899 screened in a cross-sectional descriptive study [24]. Elsewhere, mobile chest X-ray screening events (in camps) that screened a total of 1,214,289 individuals (from 2017 to 2021) detected 7,625 cases of intrapulmonary TB and patients successfully treated [25]. These findings agree with an epidemiological analysis of historical data on mass chest X-ray screening conducted in 2024, demonstrating a major and sustained reduction in TB case notifications [26]. In the studies of [27], mobile X-ray targeted screening for TB resulted in an overall yield of 200 per 100,000 persons screened, with a focus at homeless persons and problem drug users. This proves that targeted active case finding using X-rays has the potential to deliver a major contribution to intrapulmonary TB. Despite several positives, this approach has been reported to suffer logistics and funding challenges, impacting successful TB program implementation across the globe especially in low resource settings [24, 28].

Contemporary practice in chest radiography has witnessed the creation of portable systems that prioritize convenience and accessibility, now being deployed for diagnostic and/or screening activities located far from health structures, for example, outreach interventions (see **Figure 4b**). This battery-powered and completely wireless transportable technology (weighing less than 30 kg, including all accessories) allows rapid and accurate chest X-ray services for intrapulmonary TB to be brought directly to communities and can be performed in remote locations, resource-constrained or other non-clinical settings. It possesses an energy-efficient high-frequency generator that produces image quality comparable to stationary X-ray systems and an integrated digital detector and precise collimation system; but since it is mostly not performed in a dedicated room, it will demand adequate radiation protection measures put in place, such as distance, time, and shielding [29].

Community-based screening efforts with these portable digital X-ray units, as illustrated, have shown the potential to identify people with intrapulmonary TB at a very early stage in their disease course and to substantially increase notification rates. Its emerging use in combination with AI systems is rapidly reshaping the landscape of imaging practice.

Artificial intelligence is concerned with replicating human intelligence in machines, trained to perform knowledge-intensive tasks, accomplish advanced

functions, solve problems, and make decisions. The roots of AI can be traced back to the 1940s, when the "Turing test" – a test to check the ability of a machine to exhibit intelligent behavior equivalent to human intelligence – sparked the first AI conference held at Dartmouth College. McCarthy's AI programming language (LISP), Weizenbaum's interactive natural language processing (NLP) computer program (ELIZA), and Shakey, the mobile robot, were notable achievements between the 1940s and 1970s, which laid the foundation for the discovery of expert systems (ES) (knowledge-based systems MYCIN and EMYCIN), algorithms, machine learning (ML), and deep learning (DL) from the 1970s to the 2020s. Later advances have seen AI systems being able to process vast amounts of data to make accurate predictions and generate images, texts, videos, and 3D designs in response to prompts. This is known as generative AI (GenAI), rooted in the GPT (generative pre-trained transformer) architectural foundation and built into different language models such as GPT-1, GPT-2, GPT-3, and GPT-4. GenAI continues to learn and evolve, using neural networks to identify patterns and undergoing training on large unlabeled datasets to predict outcomes in the same ways humans act [30].

In the field of medical imaging, the ability of these computer systems to learn to identify complex patterns and trends in radiographic images and reports (via feature learning techniques, artificial neural networks [ANNs], NLP, etc.) without constant guidance from humans is the reason behind AI's successful integration with imaging technologies. They are able to extract features from images, identify abnormalities, and generate reports. Chest X-ray–compatible AI-powered computer-aided detection (CAD) software solutions (such as CAD4TB [Delft Imaging], INSIGHT CXR [Lunit], and qXR [Qure.ai]) have been able to solve intra and inter-reader variability of CXR reporting and the challenging nature of precise adherence of human readers to guidelines on CXR interpretation by providing reports in a few seconds/minutes that are consistent, adaptable, and unaffected by fatigue, stress, or lapses of concentration. AI-powered portable X-ray systems could be deployed either in the form of cloud-based solutions or offline systems. The cloud-based option is cheaper, quicker to troubleshoot, and easier to upgrade to new services/software versions, and it can be accessed by a central expert radiologist for quality control, although it is dependent on stable internet connections with high upload bandwidth and may experience downtime, resulting in major delays in screening practices, particularly when not used in conjunction with an on-site human reader. The offline category does not need an internet connection and can be very useful for screening in remote areas that lack stable internet, but it requires expensive laptops with high-end computing and graphical processing power; also, installation and maintenance can be cumbersome. Nevertheless, a key consideration will be the availability of information technology (IT)/human resources for support as well as skilled personnel to conduct CXR examinations, maintain the equipment, and read the results [31–33].

This AI feature has significantly increased the diagnostic capacities of the system, its efficacy and efficiency, and its appropriateness and advantages of use, as seen in the latest studies. Abiola, in 2025, with the aim of bringing pulmonary TB screening innovations to hard-to-reach communities and strengthening the active case-finding interventions for TB, demonstrated an average presumptive TB proportion of 10.84 ± 5.42% and 10% confirmed TB cases from 94,694 subjects screened using ultra-portable digital X-ray with CAD4TB [34]. Similarly, a Delft-light backpack portable digital X-ray CAD4TB unit identified 1,140 (13.9%)

presumptive TB cases out of a total of 8,230 participants screened for PTB, with the proportion of confirmed TB cases given as 12.0% and 5.6% for men and women, respectively ($P < 0.001$) [35]. The evaluation of the ultra-portable X-ray system revealed its significant potential to improve PTB case detection and equitable access to high-quality TB care, producing a mean image quality rating of 3.71 (compared to a reference of 3.99, $P < 0.001$) with no significant differences in TB abnormality scores, nor in any of the steps along the TB care cascade during campaigning [36]. In a comparative study of ultra-portable CXR screening to TB symptom screening in campaigns, it was found to provide more efficient TB screening in hard-to-reach areas, with the AI feature able to improve triaging when human readers are unavailable and save expensive diagnostic testing costs [37]. According to a recent formative assessment in 2024, the implementation of a portable digital chest X-ray machine at the community level is the best means for PTB screening/contact tracing, allowing for more TB contacts living with the index patient to be screened without proximity and transportation constraints [38]. In a further literature review, the heterogeneity of active TB risk among population groups was noted, indicating that systematic chest X-ray-led screenings should be targeted at specific high-risk groups rather than universally applied to optimize PTB yield [39].

Chest radiography contains a large amount of information about a patient's health and has great clinical value in the diagnosis of a range of chest anomalies. Radiographic findings associated with active intrapulmonary TB (**Figure 5a–d**) are [40–42]:

(1) *Airspace disease:* Infiltration, consolidation, or opacification of lung parenchyma involving any lung segment or lobe (Ghon focus) and silhouetting adjacent structures, including caseating granuloma (also known as a tuberculoma, representing a pulmonary nodule), which typically calcifies, becoming a Ghon lesion.

(2) *Lymphadenopathy*: Chest X-ray is usually unremarkable during the incubation stage (CT preferred) but typically presents with lobulated hilar/paratracheal opacity. There is potential for airway attenuation or deviation. A doughnut sign may be observed on a lateral radiograph. Airway compression or displacement is the most reliable finding. Attenuation can result in distal ipsilateral hyperinflation, atelectasis, or consolidation.

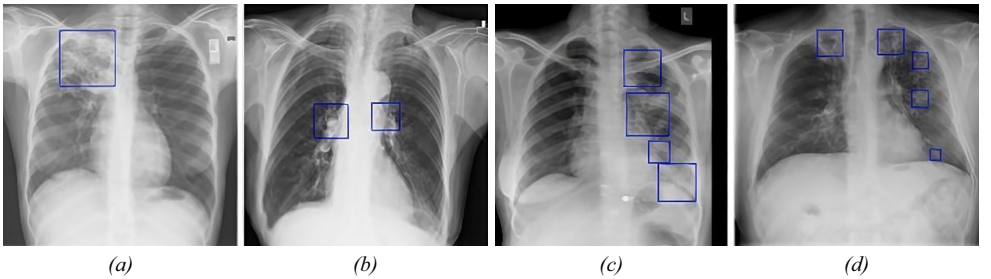

Figure 5.
Primary and post-intrapulmonary tuberculosis appearance on a chest X-ray.

(3) *Cavitation*: Cavity formation is the hallmark of postprimary TB. Small cavities are easily missed on CXR, as it is often difficult to distinguish a small cavity from consolidation. Airspace opacification surrounding an area of cavitation represents central caseous necrosis and liquefaction. An air-fluid level may represent secondary infection.

(4) *Miliary TB:* Chest X-ray is usually unremarkable at the onset but manifests as diffuse small non-calcified/sarcoid nodules (1–3 mm to 5 mm in diameter, randomly distributed throughout both lungs with a "snow-storm" appearance) with intra and interlobular septal thickening. Computed tomography is able to demonstrate miliary disease before it becomes radiographically apparent. This miliary pattern, well-defined, uniformly distributed, and representing hematogenous dissemination, is different from the tree-in-bud nodules seen under bronchiectasis below, which have a patchy distribution and are poorly defined.

(5) *Pleural effusion*: Increased homogeneous density superimposed over the lung fields, more commonly seen in 30–40% of adult cases and 5–10% of pediatric cases.

Chest X-ray is a vital and preferred imaging technique employed to monitor intrapulmonary TB treatment and clinical outcomes, such as response to characteristic features like infiltrates, cavitation, effusion, lymphadenopathy, and miliary pattern (see **Figures 6**, **7** and **Table 1**). Repeated tissue damage and repair often result in pulmonary fibrotic scarring, linear opacity, calcifications, or volume loss on CXR even after treatment [43].

4.2 Computed Tomography

Computed tomography is the method of choice to reveal early bronchogenic spread in postprimary intrapulmonary TB and is more sensitive than CXRs in detecting lymphadenopathy and characterizing the infection as active or not. A CT scan combines a series of X-rays to create cross-sectional, detailed gray-scale images of internal structures in the chest region that represent the distribution of X-ray attenuation coefficients. Images obtained through 360 degrees then undergo reconstruction into three primary planes – axial, coronal, and sagittal – from a single 3D dataset, allowing for detailed multiplanar views of the anatomy [44].

A CT machine is very bulky and expensive and requires on-site installation. Most importantly, it involves a much higher dose of radiation (5–7mSv) compared to a standard CXR (0.1mSv), which poses a greater health risk, especially for routine screening, making it impractical for widespread screening. Again, CT alone lacks the sensitivity and specificity required for accurate intrapulmonary TB diagnosis due to overlapping imaging features with other conditions like lung cancer, leading to misdiagnosis, and is therefore not recommended for routine use [45, 46].

It is, therefore, not recommended for initial mass screening but is useful in certain clinical situations (see **Figures 8–10** and **Table 2**) [42, 47, 48]:

(1) *Lymphadenopathy:* Right paratracheal and hilar lymph nodes are the most common sites of nodal enlargement (>2 cm), with a "rim sign," consisting of

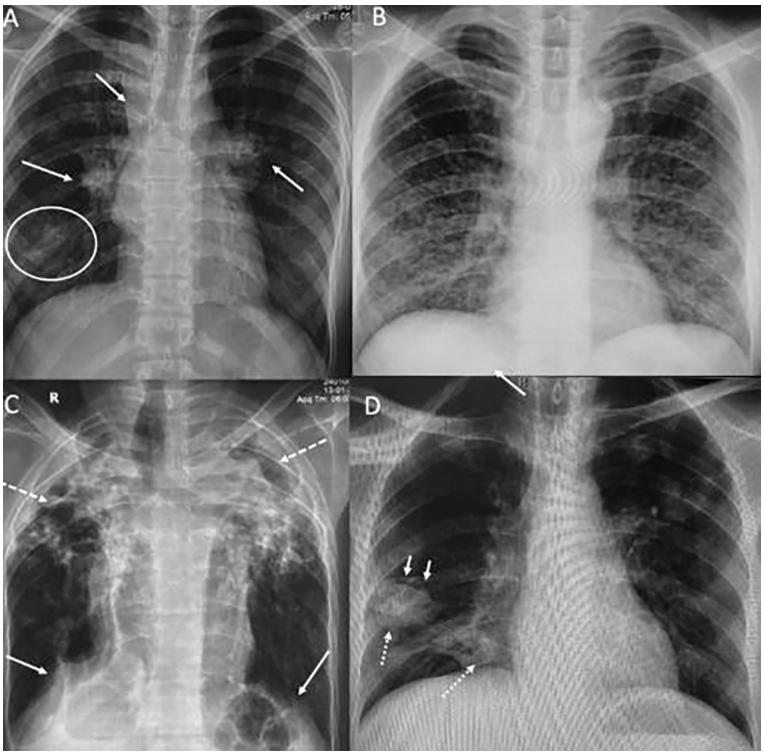

Figure 6.
Chest X-ray in PTB.

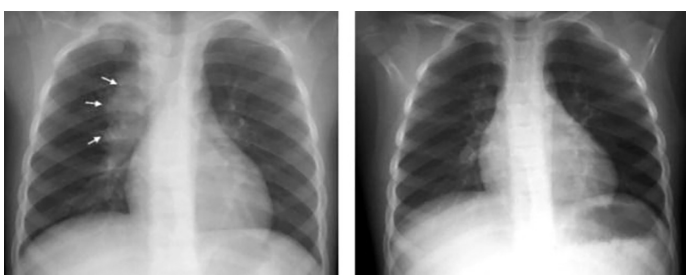

Figure 7.
Right paratracheal and hilar lymphadenopathy before and after treatment.

1	Patches of consolidation
2	Centrilobular nodules (tree-in-bud appearance)
3	Miliary nodules
4	Cavitation
5	Lymphadenopathy
6	Fibro-cavitary changes and pleural effusion

Table 1.
Summary of CXR findings.

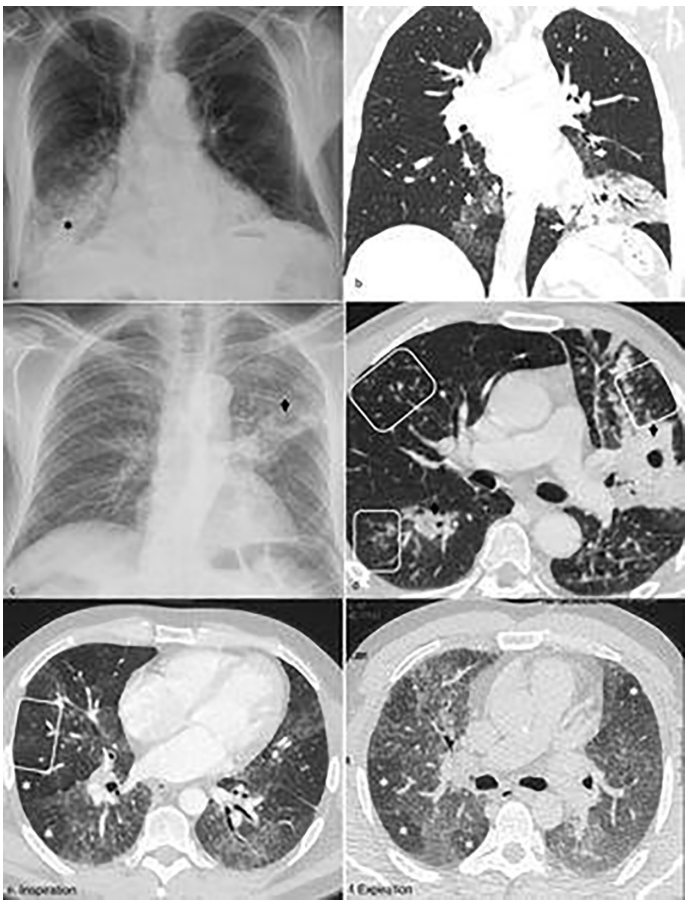

Figure 8.
Multifocal pulmonary opacities.

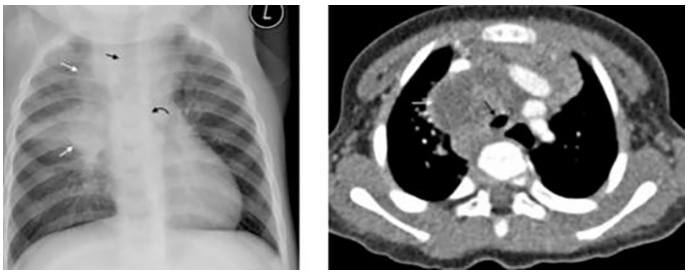

Figure 9.
Imaging comparison on CXR and CT of same patient.

a low-density center representing caseous necrosis, surrounded by a peripheral enhancing rim due to granulomatous inflammatory tissue. Contrast-enhanced CT delineates lymph nodes and shows central necrosis well, along with peripheral rim enhancement. It allows accurate assessment of

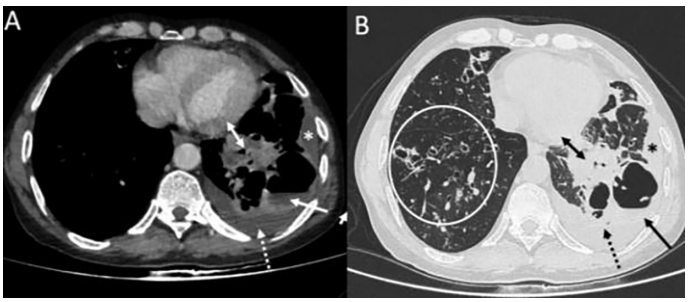

Figure 10.
PTB CT chest windowing alt- text: (a) Axial mediastinal and (b) lung window sections denoting cavities with air-fluid levels in left lower lobe, consolidation, associated pleural effusion and bronchiectatic changes encircled in right lower lobe.

1	Location	Upper lobes, superior segments of the lower lobes, subpleural consolidation
2	Nodules	Centrilobular (tree-in-bud), miliary, peri-lymphatic
3	Lymph nodes	Hilar and mediastinal, calcified, central necrosis (rim sign), enhancing
4	Pleural involvement	Pleural effusion, empyema, bronchopleural fistula

Table 2.
Summary of CT findings.

lymph node compression, measurement of stenosis length, and prediction of whether the offending node is endobronchial, submucosal, or peri-bronchial.

(2) *Bronchiectasis:* Early bronchogenic spread in CT appears as 2–4-mm centrilobular nodules (inflammatory lesions in the bronchioles and peribronchial alveoli) and sharply marginated linear branching opacities around terminal and respiratory bronchioles (tree-in-bud sign). This sign mimics the branching pattern of a budding tree, and an increased broncho-arterial ratio (severely dilated bronchial lumens or bronchial wall thickening, leading to increased broncho vascular markings) is indicative of bronchiectasis.

(3) *Differentiation between active and latent PTB:* While chest radiographs may show mild or nonspecific findings in patients with active PTB, studies reveal that CT scans can correctly diagnose 91% of cases of PTB and correctly characterize 80% of patients with active disease and 89% with inactive disease. Features include cavitation/cavity lesions, clusters of nodules, presence of centrilobular nodules, and consolidation involving the apex, the superior segment of the right or left lower lobe, or the posterior segment of the right upper lobe or left upper lobe.

Computed tomography provides insights into postprimary intrapulmonary TB/treatment, such as the response to parenchymal, airway, pleural, mediastinal, and vascular sequelae of intrapulmonary TB (although CXR, to some extent, can reveal

Figure 11.
Imaging comparison on CXR and CT of same patient presenting with PTB.

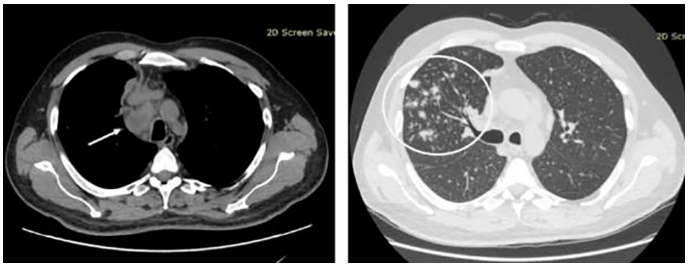

Figure 12.
Follow-up CT after eight weeks of treatment.

some of these features) (see **Figures 11** and **12**). These include calcified mediastinal or hilar masses with central airway narrowing, mediastinal lymphadenopathies, early bronchogenic spread, bronchial obstruction secondary to fibrosis (which may result in obstructive pneumonia or atelectasis), pulmonary vessel encasement, and compression of the superior vena cava [49].

4.3 Positron emission tomography–computed tomography

Is a hybrid form of imaging in nuclear medicine that involves the injection of a radioactive compound such as F-18 Choline, Ga68 PSMA, F-18 Choline, F-18 PSMA, C11 Methionine, ^{18}F-FDG (18F-fluorodeoxyglucose, most common) into the body, which undergoes decay to produce two 511 KeV gamma photons following annihilation, detected externally with a PET scanner. This imaging method provides both anatomic and metabolic information and is widely used for the differentiation of malignant from benign lesions, including identifying patients at high risk of relapse. It works by the accumulation of ^{18}F-FDG in inflammatory cells such as neutrophils, activated macrophages, and lymphocytes at the site of inflammation or infection; these signals are detected as ^{18}F-FDG uptake, usually seen in intrapulmonary TB, in tuberculoma, and in other TB-related lesions [50].

Several studies have demonstrated the relevance of PET/CT in assessing the response to intrapulmonary TB treatment (although it can mimic lung cancer), owing to its high sensitivity in detecting and assessing disease activity,

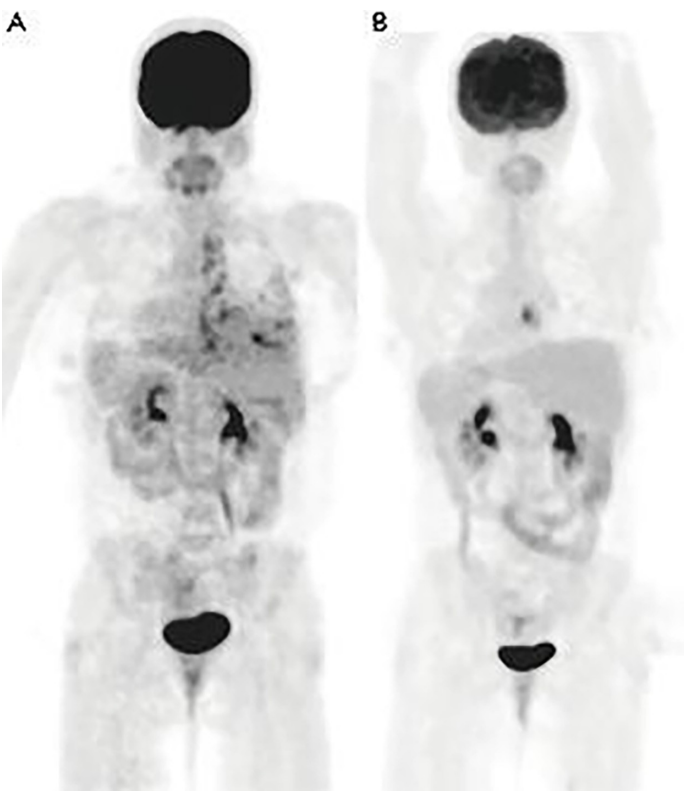

Figure 13.
Whole-body PET scan.

inflammation, response to therapy, and malignancy (see **Figures 13** and **14**). However, it is not for routine use and involves high radiation exposure.

Chen [51], in a prospective study, discovered bronchial spread of PTB, primarily from cavities but occasionally from consolidations, with PET/CT displaying 17% new or expanding lesions linked to cavities via bronchial inflammation that were not present at baseline.

Active PTB shows increased ^{18}F-FDG uptake with high standardized uptake values (although it may mimic cancer). Evaluating FDG/PET-CT studies assessing response to treatment in a recent review in 2024 [52, 53] showed a decrease of 31% in ^{18}F-FDG standardized uptake value after one month of treatment. This finding seems consistent with [54], where a reduction in the total glycolytic activity index by 30–62% at four weeks of treatment in cured patients was observed. With treatment, this translates to a reduction in standardized uptake value max as noted in [55]. On the contrary, the standardized uptake value in nonresponders to TB treatment was higher after four months, outperforming lymph node size in predicting nonresponders ($P < 0.01$) [56], which agrees with studies where baseline standardized uptake value and the number of lymph node regions involved were higher in treatment nonresponders [52].

Predicting unfavorable outcomes or recurrent infections is another aspect. Treatment failure was reflected by the failure to reduce the total glycolytic activity

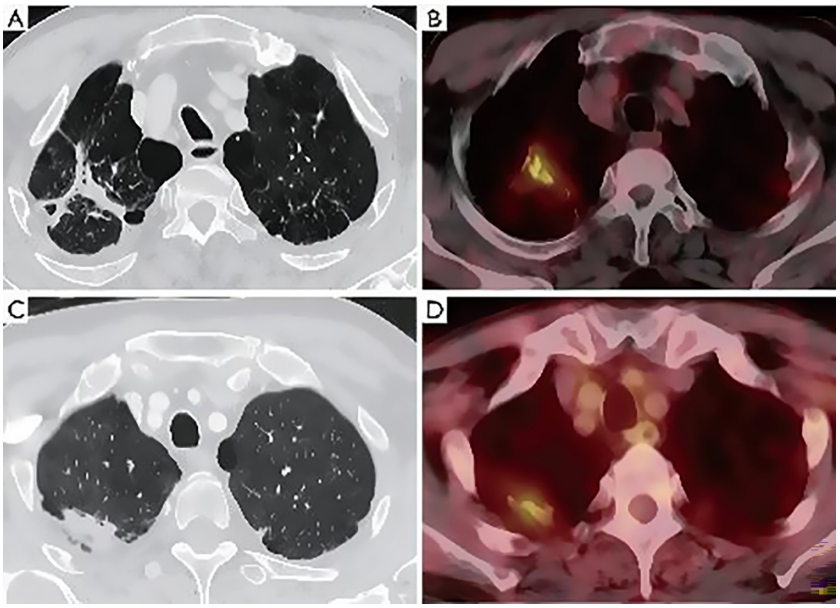

Figure 14.
Previously healed PTB: CT and 18F-FDG-PET/CT imaging comparison among two subjects.

index by < 80% at the end of treatment (EoT) in 2020 [57]. In cases requiring a longer duration of treatment and higher chances of mortality, nonresponse at 12 weeks following PET/CT imaging was observed [58]. Persistent metabolic activity at EoT may signal metabolically active old lesions (not active); thus, correlation with clinical data is essential when assessing EoT [59].

4.4 Ultrasound

Ultrasound, though portable, cost-effective, and radiation-free, lacks sufficient evidence regarding its appropriateness as a diagnostic imaging method for intrapulmonary TB. Nevertheless, studies have reported its useful role in identifying pleural effusions and guiding minimally invasive interventional procedures, such as the placement of chest tubes, drainage of loculated collections, thoracentesis, and percutaneous biopsy of subpleural pulmonary consolidations or pleural plaques [60].

5. AI techniques in imaging of intrapulmonary TB (workflow, triaging, prioritization, diagnosis, dose reduction, image quality, reporting, and treatment outcome prediction) and concerns

Artificial intelligence is a set of technologies that empowers intelligent computers to learn, reason, and perform a variety of advanced tasks in ways that used to require human intelligence, utilizing certain techniques, methods, and algorithms to successfully carry out knowledge-intensive tasks. Artificial intelligence use in intrapulmonary TB diagnosis/management is rapidly

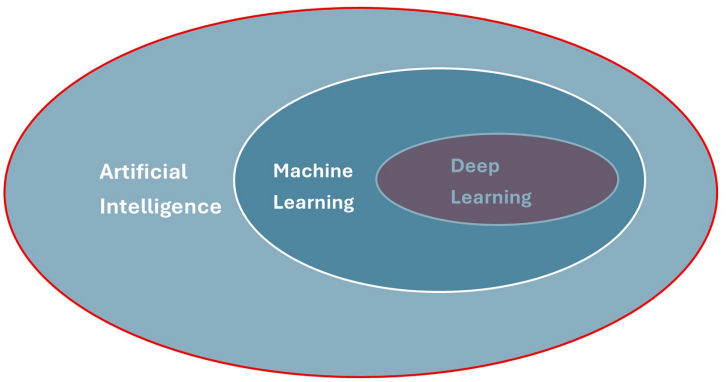

Figure 15.
Artificial intelligence and major domains.

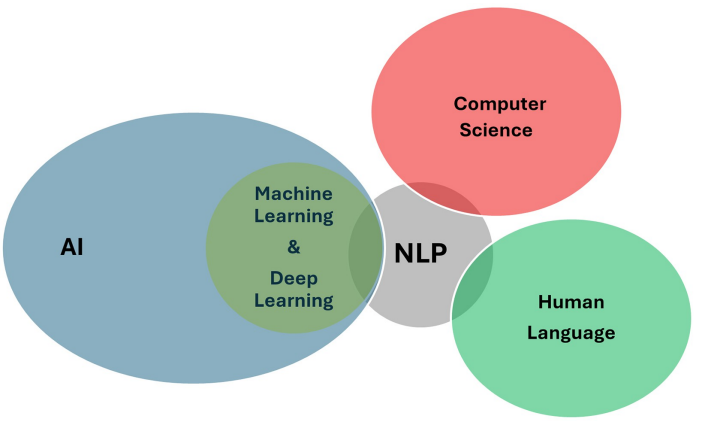

Figure 16.
Natural language processing and components.

evolving, employing techniques such as ML, DL, NLP, ES, fuzzy logic (FL), and robotics. However, ML and DL appear to be the most used due to their robust performance (see **Figures 15** and **16**).

5.1 Machine learning

Machine learning is powered by "algorithms," which inform the computer how to learn to operate on its own. These algorithms are the step-by-step instructions that enable an intelligent system to complete a task and are divided into three major types (supervised, unsupervised, and reinforcement learning) based on the learning process involved to make predictions. Supervised learning entails humans acting as a guide, training the model on a labeled dataset on predefined tasks, for example, classification (predicting distinct class labels) and regression (predicting a continuous quantity). In unsupervised learning, the computer learns from an unlabeled dataset with no defined output to identify complex processes and patterns

in the absence of constant guidance from humans, for example, cluster analysis and feature learning tasks (feature extraction and feature selection). Reinforcement learning, on the other hand, is characterized by the absence of both human intervention and a training dataset, as the system learns from its experience through repeated trial and error [30].

In imaging and management of PTB, ML algorithms (supervised and unsupervised), as seen in studies, play vital roles in workflow, diagnosis, prediction, and dose reduction. Popular ML models that carry out these tasks include k-nearest neighbors (KNN), support vector machine (SVM), decision tree (DT), hierarchical clustering, random forest (RF), k-means clustering, logistic regression, and naive Bayes (NB) [61–63]. A brief description of these models is given in **Table 3.**

As seen in a practical case study on PTB screening [64], an AI-integrated queue management system driven by advanced algorithms was extremely useful in workflow, worklist management, and crowd control, promoting orderliness, accuracy, communication, and maintaining privacy. These parameters are vital in

ML model	Type and function	Role in PTB imaging
K-nearest neighbors (KNN)	Supervised; classification and regression	Classifies a pixel or region (e.g., a lung nodule) based on the majority class of its "k" closest neighbors (already labeled images) in the feature space and averages values for regression
Support vector machine (SVM)	Supervised; classification and regression	Robust classification by finding the best "hyperplane" (decision boundary) to separate TB-positive features from healthy lung features, also extended to regression
Decision tree (DT)	Supervised; classification and regression	Tree-like model of decisions (e.g., "Is the nodule solid? Is it calcified?") to classify regions/discrete classes and continuous values (regression) by choosing different splitting criteria; also useful for interpretability
K-means clustering	Unsupervised; clustering and feature learning	Partitions data points into a predefined number of clusters (k), where each data point belongs to the cluster with the nearest mean (centroid); useful in CXR image segmentation, feature analysis, and as a component in CAD automated diagnostic systems
Hierarchical clustering (HCA)	Unsupervised; clustering and feature learning	Builds a hierarchy of clusters and does not require the number of clusters to be specified beforehand, offers natural groupings within complex image data (e.g., various subgroups of radiographic presentations of PTB), correlates severe pulmonary radiological manifestations with clinician data, facilitates feature extraction, and enhances advanced deep learning models
Random forest (RF)	Supervised; classification and regression	Ensemble of many decision trees by averaging predictions from individual trees for regression and taking the majority vote for classification, thus improving robustness and accuracy, making it strong at handling noisy PTB CXR image data
Logistic regression	Supervised; classification and regression	Classifier that extracts image features to predict the probability of PTB presence and odds ratios
Naïve Bayes (NB)	Supervised; classification and regression	Uses probability (Bayes' theorem) to predict disease and classification and is good for text-based or feature-rich PTB data

Table 3.
Description of popular ML models.

improving the quality of care and clinical outcomes, owing to the highly infectious and widespread nature of the disease. Elsewhere [65], an ML algorithm (XmarTB tool) reportedly yielded a sensitivity of 98.1% and specificity of 99.7% in detecting PTB cases among abnormal CXRs, as well as a sensitivity of 96.7% and specificity of 98.7% in detecting PTB cases among all CXRs, proving to be an accurate diagnostic tool in automatically detecting abnormal CXRs and satisfactorily differentiating PTB from other thoracic diseases. This is consistent with the studies of [66], where a similar CAD software (comprising image preprocessing, extracting region of interest [ROI] regions, extracting ROI features, and classifying disease according to the features) enhanced CXR interpretation and resulted in the discovery of more PTB patients during community screening initiatives. In addition, the use of noise reduction algorithms has achieved dose reductions of approximately half (47.8%) in CXR without compromising image quality for abnormal lung findings [11]. Furthermore, ML models (DT) were useful in predicting PTB treatment success and adverse effects (accuracy – 92.72%, AUC – 0.909, precision – 95.90%, recall – 95.60%, and F1-score – 95.75%), thus improving PTB management [67]. However, as radiological data continues to increase disproportionately in comparison with trained readers, determining in a robust way features for PTB as well as other chest abnormalities has opened up opportunities for advancing traditional CAD systems in imaging, leading to deep learning.

5.2 Deep learning

Deep learning entails the use of "artificial neural networks", which comprise several processing layers to learn from data, mimicking the way the brain processes information. Examples of common DL algorithms are multilayer perceptron (MLP), convolutional neural networks (CNNs), long short-term memory networks (LSTMs), recurrent neural networks (RNNs), generative adversarial networks (GANs), and Autoencoder. Convolutional neural network is the most widely used DL algorithm, consisting of a convolutional layer (feature extraction), pooling layer (feature selection), and connected layer (integrates extracted features), which has been excellent in diagnosis, triaging/prioritization, and dose reduction in PTB imaging (see **Figure 17**) [60]. **Table 4** describes these algorithms [68–70].

As demonstrated in the experimental studies of [71], an AI system based on CNNs (incorporating NLP) successfully automated real-time triaging of adult CXR on the

Figure 17.
DL model- PTB in CXR.

DL algorithms	Description	Role in PT imaging
Multilayer perceptron (MLP)	Fully connected network consisting of an input layer, one or more hidden layers, and an output layer, utilizing the backpropagation technique	Basic detection and classification tasks in PTB struggle with complex spatial patterns compared to CNNs
Convolutional neural networks (CNNs)	Comprise convolutional layers (feature detection and extraction), pooling layers (feature aggregation), and connected layers (feature integration)	Excel at spatial feature extraction (lesions, opacities) in PTB diagnosis, segmenting lung fields, classifying disease severity, and dose reduction
Recurrent neural networks (RNNs) and Long short-term memory networks (LSTMs)	Consist of a generator (creates content) and a discriminator (checks for accuracy) in processing sequential data and capturing temporal patterns	Sequential data, like changes over time or time-series scans, crucial for tracking PTB disease progression and treatment response in follow-up scans (with LSTMs handling longer dependencies better) and predicting future disease states
Generative adversarial network (GAN)	Comprises of input, hidden layers (for remembering information), and output	Data augmentation and image enhancement, for example, generating synthetic PTB X-rays to balance datasets and creating high-quality images for better model training
Autoencoder	Feedforward neural network, made up of the encoder, the code, and the decoder trained to repeat data from the input to the output layer	Feature extraction/compression, capturing essential features with minimal data loss, dose reduction, image enhancement, and PTB anomaly detection

Table 4.
Description of popular DL models.

basis of the urgency of imaging appearances (critical, urgent, nonurgent, or normal), recording sensitivity, specificity, positive predictive value, and negative predictive value of 71%, 95%, 73%, and 94%, respectively. A feature that can be incorporated during mass screening programs further reduced the average reporting delay time from 11.2 to 2.7 days for critical imaging findings ($P < 0.001$) and from 7.6 to 4.1 days for urgent imaging findings ($P < 0.001$). A similar deep neural network was found to be non-inferior to radiologists for active pulmonary TB triaging in a population with a high TB burden ($P < 0.001$) [72].

The use of recent DL-based models for accurate and precise detection of PTB in CXR achieved classification accuracy, precision, recall, F1-score, and AUC values of 99.29%, 99.30%, 99.29%, 99.29%, and 0.999, respectively, asserting the system's efficacy and superiority to clinicians' precision in PTB diagnosis [73].

Evaluation of three popular DL systems (CAD4TB, Lunit INSIGHT, and qXR) for PTB detection in CXR TB programs achieved similar AUC values (CAD4TB [0.92, 95% CI: 0.90–0.95], Lunit [0.94, 95% CI: 0.93–0.96], qXR [0.94, 95% CI: 0.92–0.97]) with significantly higher sensitivity than radiologists (except one), further reducing by 66% the number of Xpert MTB/RIF confirmation tests for PTB, which is the gold standard, while also maintaining sensitivity at 95% or better [74]. The findings of [75] noted a nearly perfect AUC (0.99) for PTB in CXR.

An integrated DL model, upon evaluation in PET/CT, yielded hugely promising results (AUC 0.84 [0.82–0.88], sensitivity 0.85 [0.80–0.88], and specificity 0.84

[0.83–0.87]) in distinguishing PTB nodules from lung cancer based on DL features, radiomic features, and clinical information [76].

In chest CT, there was no statistically significant difference between the deep learning CNN model and the physicians in detecting PTB [77]. Interestingly, another study proved that the mean effective radiation dose of ultra-low-dose CT following DL algorithm use (CycleGAN) was 0.12 mSv, with a mean 93.9% reduction compared to standard-dose CT, still producing quality images [78].

5.3 Natural language processing

Natural language processing (NLP) is an AI technique that understands and processes human language development in the form of texts or spoken words (historically focused on English due to larger datasets, but significant advances are now happening with multilingual tools such as translation and chatbots). Natural language processing comprises natural language understanding (NLU), which understands the arrangement of words and sounds, and natural language generation (NLG), which produces sentences. NLP in PTB imaging has applications across dataset creation, report generation, diagnosis, and assistance in clinical decision-making [60].

Natural language processing has been used to generate captions for abnormal CXR (pulmonary diseases such as PTB) in 283 seconds (consistent with the radiologist's report), which provides prior information for writing reports and making CXR interpretation more efficient [79]. Natural language processing (embedded into deep CNN) also generated reports of lung diseases (TB) from CXR, achieving an accuracy of 94% [80]. In addition, an NLP model discovered PTB in an incidental lung nodule (ILN) follow-up program on a CT scan, which produced positive acid-fast bacilli (AFB) testing and a positive culture for pan-susceptible *Mycobacterium tuberculosis*, prompting initiation of treatment [81].

5.4 Expert system

Expert system refers to a computer program that learns by accumulating knowledge and integrates it with a set of rules (inference rules engine) to make decisions; the main components are the knowledge base, inference engine, and user interface. It is mostly used in conjunction with ML/DL systems to improve accuracy. In the research of Zulkifli et al. [82], they developed InceptionV3, a lung disease diagnosis expert system (built on CNN and SVM architecture), which uses human knowledge to diagnose lung TB (including other lung diseases) in CXR. It produced one of the best results – classification accuracy, precision, recall, and F1-score were 0.86, 0.91, and 0.91, respectively.

5.5 Robotics

It is a system in which robots are conditioned to carry out certain tasks without any further human intervention. Excellent results in robotic-assisted lung resection surgery on patients with advanced intrapulmonary TB have been observed, demonstrating the efficacy and safety of using robots in standard lobectomy with pulmonary TB [83]. Elsewhere, robot-assisted thoracoscopic (RATS) bi-lobectomy

for PTB yielded very impressive results with a one-year follow-up, reducing some limitations of video-assisted thoracoscopic surgery (VATS) [84].

5.6 Fuzzy logic

Fuzzy logic is rooted in approximate reasoning and decision-making, applied in situations where true or false cannot be ascertained. It comprises four parts as follows:

(1) *Rule base*: It contains all rules and conditions to control decision-making.

(2) *Fuzzification*: It converts crisp input into fuzzy sets.

(3) *Inference engine*: It checks for the degree of match between fuzzy inputs and rules

(4) *Defuzzification*: It converts fuzzy sets to crisp output.

Recently, in 2024, a novel fuzzy lattice (formed using X-ray image pixels and lattice kinetic energy (K.E.) assisted EJAYA Q-Learning, utilizing a classifier for the automatic detection of pulmonary TB (presence or absence)) remarkably achieved accuracy, sensitivity, specificity, precision, and F-score of 95.50%, 96.39%, 94.40%, 95.52%, and 95.95%, respectively. When compared with contemporary classification techniques, it showed superiority in terms of accuracy (96.928% and 95.905% for presence and absence of PTB, respectively) and speed of classification (39.98 seconds) [85].

The use of AI effectively and safely in PTB imaging requires a thoughtful and cautious approach, acknowledging that while AI offers immense potential, it also presents significant risks, ranging from data privacy issues, security concerns, cost/hardware limitations, algorithmic biases, information accuracy and reliability challenges, and ethical and regulatory ambiguities. It is important to anonymize data where possible, adjust privacy settings (e.g., access, deletion, restrict data processing), educate patients on informed consent for data sharing, and implement strong cybersecurity measures. Again, training models on large, quality, and diverse datasets will boost accuracy, robustness, and generalizability. Issues regarding transparency, explainability, accountability, human oversight, and regulatory frameworks need to be addressed. Above all, interdisciplinary collaboration, stakeholder engagement, AI literacy, external funding for AI research, and continuous professional development training are required to effectively integrate AI into imaging practice, understanding its capabilities and limitations [11, 30].

6. Conclusion

Medical imaging plays a critical role in the screening, diagnosis, treatment, and management of intrapulmonary TB; AI applications are rapidly gaining momentum and enthusiasm for their utilization due to impressive results. However, rigorous validation of AI models, as well as ethical considerations, must be in check to guarantee responsible AI use.

Author details

Victor Chigbundu Nwaiwu*
School of Health and Rehabilitation Sciences, Department of Radiography, Health Sciences University, Bournemouth, United Kingdom

*Address all correspondence to: victor.chigbundunwaiwu@hsu.ac.uk

IntechOpen

References

[1] Kashif M, Nayer M, Shoukat A, Ullah A, Sheema HN, Ullah J, Slim M, Ullah A. Clinical validation of GeneExpert MTB/RIF Assay in the rapid diagnosis of extra pulmonary tuberculosis. Bulletin of Biological and Allied Sciences Research. 2024;**9**(83): 1–5. DOI: 10.54112/bbasr.v2024i1.83

[2] Shuoyi Y, Bin L, Xinyue H, Yun T, Kun L, Meng H, Bohan W, et al. Diagnostic value of microRNAs in active tuberculosis based on quantitative and enrichment analysis. Diagnostic Microbiology and Infectious Disease. 2024;**108**(4):116720. DOI: 10.16/j.diagmicrobio.2024.116172

[3] Fatima AHM, Israa AJA, Kais KAL, Ahmed AJA. Pulmonary tuberculosis risks and challenges. E3S Web of Conferences Aquaculture. 2023;**381** (01101):2–5. DOI: 10.1051/e3sconf/202338101101

[4] World Health Organization (2025) Tuberculosis. Available from: https://www.who.int/news-room/fact-sheets/detail/tuberculosis#:~:text=A%20total%20of%201.25%20million,Sustainable%20Development%20Goals%20(SDGs) [Accessed: 2025-September-27]

[5] Omoteso OA, Fadaka AO, Walker RB, Khamanga SM. Innovative Strategies for Combating Multidrug-Resistant Tuberculosis: Advances in Drug Delivery Systems and Treatment. Microorganisms. 2025;**13** (4):722. DOI: 10.3390/microorganisms13040722

[6] World bank (2025) Why is the fight against tuberculosis far from over? The answer in four charts. Available from: https://datatopics.worldbank.org/world-development-indicators/stories/why-is-the-fight-against-tuberculosis-far-from-over.html#:~:text=Incidence%20of%20tuberculosis%20(per%20100%2C000%20people)&text=Without%20treatment%20about%20half%20of,percent%20between%202015%20and%202025.[Accessed: 2025-September-27]

[7] Tran XT, Duong KL, Bui DM, Dang KL, Hoang NT, Bui TH, Gautret P, Dao TL, Hoang VT. High prevalence and risk factors of positive sputum smear in newly diagnosed pulmonary tuberculosis patients in Vietnam. Infezioni in Medicina. 2025;**33**(2): 212–220. DOI: 10.53854/liim-3302-7

[8] Chigbundu Nwaiwu V, Kanti Das S. AI-assisted abnormal CXR findings and correlation with behavioral risk factors: A Public Health Radiography approach to formulating policies and effective interventions. LatIA. 2025;**3**:323. DOI: 10.62486/latia2025323

[9] Inge AH, Maadrika MNP, Tjitske SR, Josje A, Jouke TA, Ludo FM, Bart B, et al Ultra-low-dose CT versus chest X-ray for patients suspected of pulmonary disease at the emergency department: A multicentre randomised clinical trial. Thorax. 2023;**78**:5

[10] Ankrah AO, van der Werf TS, de Vries EF, Dierckx RA, Sathekge MM, Glaudemans AW. PET/CT imaging of Mycobacterium tuberculosis infection. Clinical and Translational Imaging. 2016;**4**:131–144. DOI: 10.1007/s40336-016-0164-0

[11] Nwaiwu VC, Das SK. Emerging multifaceted application of artificial intelligence in chest radiography:

A narrative review. Journal of Medical Artificial Intelligence. 2024;7:39. DOI: 10.21037/jmai-24-67

[12] Coussens AK, Zaidi SMA, Allwood BW, Dewan PK, Gray G, Kohli M, Kredo T, Marais BJ, Marks GB, Martinez L, Ruhwald M, Scriba TJ, Seddon JA, Tisile P, Warner DF, Wilkinson RJ, Esmail H, Houben RMGJ. International Consensus for Early TB (ICE-TB) group. Classification of early tuberculosis states to guide research for improved care and prevention: An international Delphi consensus exercise. The Lancet Respiratory Medicine. 2024;**12**(6):484–498. DOI: 10.1016/S2213-2600(24)00028-6

[13] Amitesh G, Eshutosh C, Shipra A, Naresh K, Richa A, Divyanshi R, Parul M.Latent tuberculosis diagnostics: Current scenario and review. Monaldi Archives for Chest Disease. 2025;**95**(2984):1–9

[14] Tobin EH, Tristram D Tuberculosis Overview. [Updated 2024 Dec 22]. In: StatPearls [Internet]. Treasure Island (FL): StatPearls Publishing; 2025 Available from: https://www.ncbi.nlm.nih.gov/books/NBK441916/

[15] Yayan J, Rasche K, Franke KJ, Windisch W, Berger M. FDG-PET-CT as an early detection method for tuberculosis: A systematic review and meta-analysis. BMC Public Health. 2024;**2022**:24. DOI: 10.1186/s12889-024-19495-6

[16] Vega V, Cabrera-Sanchez J, Rodríguez S, Verdonck K, Seas C, Otero L, Van de Stuyft P. Risk factors for pulmonary tuberculosis recurrence, relapse and reinfection: A systematic review and meta-analysis. BMJ Open Respiratory Research. 2024;**11**:e002281. DOI: 10.1136/bmjresp-2023-002281

[17] Narasimhan P, Wood J, Macintyre CR, Mathai D. Risk factors for tuberculosis. Pulmonary Medicine. 2013;**2013**:828939. DOI: 10.1155/2013/828939

[18] Nguyen TA, Jing Teo AK, Zhao Y, Quelapio M, Hill J, Morishita F, Marais BJ, Marks GB. Population-wide active case finding as a strategy to end TB. The Lancet Regional Health-Western Pacific. 2024;**46**:101047. DOI: 10.1016/j.lanwpc.2024.101047

[19] Chen Q, Ren N, Liu S, Qian Z, Li M, Mustapha A, Luo W, Li J, Wang W, Hao C. Prevalence of Tuberculosis among migrants under national screening programs: A systematic review and meta-analysis. Global Health Research and Policy. 2025;**10**:24. DOI: 10.1186/s41256-025-00424-y

[20] Ahmed R, Zumla A, Taylor E, Aklillu E, Ippolito G, Satta G. Perspectives on tuberculosis in migrants, refugees, and displaced populations in Europe. IJID Regions. 2025;**14**(Suppl 2):100576. DOI: 10.1016/j.ijregi.2025.100576

[21] Wąsik J, Tubbs RS, Zielinska N, Karauda P, Olewnik Ł. Lung segments from anatomy to surgery. Folia Morphologica. 2024;**83**(1):20–34. DOI: 10.5603/FM.a2023.0011

[22] Haq I, Mazhar T, Nasir Q, Razzaq S, Mohsan SAH, Alsharif MH, Alkahtani HK, Aljarbouh A, Mostafa SM. Machine Vision Approach for Diagnosing Tuberculosis (TB) Based on Computerized Tomography (CT) Scan Images. Symmetry. 2022;**14**:10. DOI: 10.3390/sym14101997

[23] Miller C, Lonnroth K, Sotgiu G, Migliori G. The long and winding road of chest radiography for tuberculosis

detection. European Respiratory Journal. 2017;**49**(5):1700364. DOI: 10.1183/13993003.00364-2017

[24] Wali A, Safdar N, Manair R, Khan MD, Khan A, Kurd SA, Khalil L. Early TB case detection by community-based mobile X-ray screening and Xpert testing in Balochistan. Public Health Action. 2021;**11**(4):174–179. DOI: 10.5588/pha.21.0050

[25] Zaidi SMA, Creswell J, Khowaja S, Khan A, Copas A, Esmail H. Detection of pulmonary tuberculosis through mobile X-ray based active case-finding in Pakistan: A retrospective analysis from programmatic screening of 1 214 289 individuals from 2017 to 2021. BMJ Global Health. 2025;**10**(7):e019133. DOI: 10.1136/bmjgh-2025-019133

[26] Mahler B, de Vries G, van Hest R, Gainaru D, Menezes D, Popescu G, Story A, Abubakar I. Use of targeted mobile X-ray screening and computer-aided detection software to identify tuberculosis among high-risk groups in Romania: Descriptive results of the E-DETECT TB active case-finding project. BMJ Open. 2021;**11**(8):e045289. DOI: 10.1136/bmjopen-2020-045289

[27] MacPherson P, Stagg HR, Schwalb A, Henderson H, Taylor AE, Burke RM, Rickman HM, Miller C, Houben RMGJ, Dodd PJ, Corbett EL. Impact of active case finding for tuberculosis with mass chest X-ray screening in Glasgow, Scotland, 1950-1963: An epidemiological analysis of historical data. PLoS Medicine. 2024;**21**(11):e1004448. DOI: 10.1371/journal.pmed.1004448

[28] Eneogu RA, Mitchell EMH, Ogbudebe C, et al. Operationalizing Mobile Computer-assisted TB Screening and Diagnosis With Wellness on Wheels (WoW)) in Nigeria: Balancing Feasibility and Iterative Efficiency. 2020. DOI: 10.21203/rs.3.rs-75513/v1

[29] Kamal R, Singh M, Roy S, Adhikari T, Gupta AK, Singh H, VV R, Panda S, AM K, Bhargava B. A comparison of the quality of images of chest X-ray between handheld portable digital X-ray & routinely used digital X-ray machine. Indian Journal of Medical Research. 2023;**157**(2&3):204–210. DOI: 10.4103/ijmr.ijmr_845_22

[30] Nwaiwu VC, Das SK. An Artificial intelligence road map to unlocking future technologies and transforming radiology practice. Medinformatics. 2025. DOI: 10.47852/bonviewMEDIN52026362

[31] Creswell J, LNQ V, Qin ZZ, Muyoyeta M, Tovar M, Wong EB, Ahmed S, Vijayan S, John S, Maniar R, Rahman T, MacPherson P, Banu S, Codlin AJ. Early user perspectives on using computer-aided detection software for interpreting chest X-ray images to enhance access and quality of care for persons with tuberculosis. BMC Global Public Health. 2023;**1**(1):30. DOI: 10.1186/s44263-023-00033-2

[32] Zhi ZQ, Tasneem N, Morten R, Claudia MD, Sifrash G, Madlen N, Jacob C, Sandra VK.A new resource on artificial intelligence powered computer automated detection software products for tuberculosis programmes and implementers. Tuberculosis. 2021;**127**(102049). DOI: 10.1016/j.tube.2020.102049

[33] Geric C, Qin ZZ, Denkinger CM, Kik SV, Marais B, Anjos A, David PM, Ahmad Khan F, Trajman A. The rise of

artificial intelligence reading of chest X-rays for enhanced TB diagnosis and elimination. International Journal of Tuberculosis and Lung Disease. 2023;**27**(5):367–372. DOI: 10.5588/ijtld.22.0687

[34] Abiola A, Sani U, Austin I, Rupert E, Aderonke A, Bethrand O, Debby N, Eze C, Chidubem O, Omosalewa O, et al. Impact of the use of the ultra-portable digital X-ray with CAD4TB for active case finding for tuberculosis in Nigeria. Frontiers in Digital Health. 2025;**7**(1):1–5. DOI: 10.3389/fdgth.2025.1559203

[35] Odume B, Chukwu E, Fawole T, Nwokoye N, Ogbudebe C, Chukwuogo O, Useni S, Dim C, Ubochioma E, Nongo D, Eneogu R, Lagundoye Odusote T, Oyelaran O, Anyaike C. Portable digital X-ray for TB pre-diagnosis screening in rural communities in Nigeria. Public Health Action. 2022;**12**(2):85–89. DOI: 10.5588/pha.21.0079

[36] LNQ V, Codlin A, Ngo TD, Dao TP, Dong TTT, HTL M, Forse R, Nguyen TT, Cung CV, Nguyen HB, Nguyen NV, Nguyen VV, Tran NT, Nguyen GH, Qin ZZ, Creswell J. Early Evaluation of an Ultra-Portable X-ray System for Tuberculosis Active Case Finding. Tropical Medicine and Infectious Disease. 2021;**6**(3):163. DOI: 10.3390/tropicalmed6030163

[37] John S, Abdulkarim S, Usman S, Rahman MT, Creswell J. Comparing tuberculosis symptom screening to chest X-ray with artificial intelligence in an active case finding campaign in Northeast Nigeria. BMC Global Public Health. 2023;**1**(1):17. DOI: 10.1186/s44263-023-00017-2

[38] Dakum P, Agbaje A, Daniel O, Anyaike C, Chijoke-Akaniro O, Okpokoro E, Akingbesote S, Anyomi C, Adekunle A, Alege A, Gbadamosi M, Babalola O, Mensah C, Eneogu R, Ihesie A, Nongo D, Adelekan A. Implementation of Portable Digital Chest X-ray Machine for Tuberculosis Contact Tracing in Oyo and Osun States, Nigeria: A Formative Assessment. Journal of Respiration. 2024;**4**(3):163–176. DOI: 10.3390/jor4030015

[39] Dooley N, Lockwood P.Systematic screening for active tuberculosis amongst refugees and asylum seekers in Western Europe: Is universal chest radiography justified? A literature review. Radiography. 2025;**31**(1):194–200

[40] Wetscherek MTA, Sadler TJ, Lee JYJ, Karia S, Babar JL. Active pulmonary tuberculosis: Something old, something new, something borrowed, something blue. Insights into Imaging. 2022;**13**(1):3. DOI: 10.1186/s13244-021-01138-8

[41] Mathur M, Badhan RK, Kumari S, Kaur N, Gupta S. Radiological Manifestations of Pulmonary Tuberculosis-A Comparative Study between Immunocompromised and Immunocompetent Patients. Journal of Clinical and Diagnostic Research. 2017;**11**(9):TC06–TC09. DOI: 10.7860/JCDR/2017/28183.10535

[42] Feyisa DW, Ayano YM, Debelee TG, Schwenker F. Weak Localization of Radiographic Manifestations in Pulmonary Tuberculosis from Chest X-ray: A Systematic Review. Sensors. 2023;**23**(15):6781. DOI: 10.3390/s23156781

[43] Nel M, Franckling-Smith Z, Pillay T, Andronikou S, Zar HJ. Chest Imaging for Pulmonary TB-An Update.

Pathogens. 2022;**11**(2):161. DOI: 10.3390/pathogens11020161

[44] Hermena S, Young M CT-scan Image Production Procedures. [Updated 2023 Aug 8]. In: StatPearls [Internet]. Treasure Island (FL): StatPearls Publishing; 2025 Jan-. Available from: https://www.ncbi.nlm.nih.gov/books/NBK574548/ [Accessed: 2025-September-27]

[45] Tang W, Xing W, Li C, Nie Z, Cai M. Differences in CT imaging signs between patients with tuberculosis and those with tuberculosis and concurrent lung cancer. American Journal of Translational Research. 2022;**14**(9):6234–6242

[46] Jung L, Dong H, Eun Y, Deog K, Hee S. Chest CT scan as an initial diagnostic method for tuberculosis infection detected by mass screening in the intermediate-burden country. European Respiratory Journal. 2019;**54**(suppl 63):A2957. DOI: 10.1183/13993003.congress-2019.PA2957

[47] Nel M, Franckling-Smith Z, Pillay T, Andronikou S, Zar HJ. Chest Imaging for Pulmonary TB—An Update. Pathogens. 2022;**11**(2):161. DOI: 10.3390/pathogens11020161

[48] Harsimran B, Ravinder K, Irwinjit K, Karan G. Imaging Spectrum in Pulmonary Tuberculosis. Indographics. 2024;**3**(2):33–43. DOI: 10.1055/s-0044-1788611

[49] Jihad AD, Hassan TM, Wajdy JA. Limbic encephalitis associated with tuberculosis mediastinal lymphadenitis. Journal of Clinical Tuberculosis and Other Mycobacterial Diseases. 2019;**18**(Pt 7):100129. DOI: 10.1016/j.jctube.2019.100129

[50] Evangelia S, Alimuddin Z, Jamshed B. Imaging in tuberculosis. International Journal of Infectious Diseases. 2015;**32**(1):87–93. DOI: 10.1016/j.ijid.2014.12.007

[51] Chen RY, Yu X, Smith B, Liu X, Gao J, Diacon AH, Dawson R, Tameris M, Zhu H, Qu Y, Zhang R, Pan S, Jin X, Goldfeder LC, Cai Y, Arora K, Wang J, Vincent J, Malherbe ST, Thienemann F, Wilkinson RJ, Walzl G, Barry 3rd CE. Radiological and functional evidence of the bronchial spread of tuberculosis: An observational analysis. The Lancet Microbe. 2021;**2**(10):e518–e526. DOI: 10.1016/S2666-5247(21)00058-6

[52] Gail BC, Jim O, Christina CC, Anthony DK, Nicholas IP. Does PET-CT Have a Role in the Evaluation of Tuberculosis Treatment in Phase 2 Clinical Trials? The Journal of Infectious Diseases. 2024;**229**(4):1229–1238. DOI: 10.1093/infdis/jiad425

[53] Martinez V, Castilla-Lievre MA, Guillet-Caruba C, et al. (18)F-FDG PET/CT in tuberculosis: an early non-invasive marker of therapeutic response. International Journal of Tuberculosis and Lung Disease. 2012;**16**:1180–5

[54] Malherbe ST, Dupont P, Kant I, et al. A semi-automatic technique to quantify complex tuberculous lung lesions on (18)F-fluorodeoxyglucose positron emission tomography/computerised tomography images. European Journal of Nuclear Medicine and Molecular Imaging Research. 2018;**8**:55

[55] Dureja S, Sen IB, Acharya S. Potential role of F18 FDG PET-CT as an imaging biomarker for the noninvasive

evaluation in uncomplicated skeletal tuberculosis: a prospective clinical observational study. European Spine Journal. 2014;**23**:2449–54

[56] Sathekge M, Maes A, D'Asseler Y, et al. Tuberculous lymphadenitis: FDG PET and CT findings in responsive and nonresponsive disease. European Journal of Nuclear Medicine and Molecular Imaging. 2012;**39**:1184–90

[57] Malherbe ST, Chen RY, Dupont P, Kant I, Kriel M, Loxton AG, Smith B, Beltran CGG, van Zyl S, McAnda S, Abrahams C, Maasdorp E, Doruyter A, Via LE, Barry 3rd CE, Alland D, Richards SG, Ellman A, Peppard T, Belisle J, Tromp G, Ronacher K, Warwick JM, Winter J, Walzl G. Quantitative 18F-FDG PET-CT scan characteristics correlate with tuberculosis treatment response. EJNMMI Research. 2020;**10**(1):8. DOI: 10.1186/s13550-020-0591-9

[58] Sood A, Mittal BR, Modi M, Chhabra R, Verma R, Rana N, Parihar AS, Satapathy S, Kumar R. 18F-FDG PET/CT in Tuberculosis: Can Interim PET/CT Predict the Clinical Outcome of the Patients? Clinical Nuclear Medicine. 2020;**45**(4):276–282. DOI: 10.1097/RLU.0000000000002968

[59] Lawal IO, Fourie BP, Mathebula M, Moagi I, Lengana T, Moeketsi N, Nchabeleng M, Hatherill M, Sathekge MM. ^{18}F-FDG PET/CT as a Noninvasive Biomarker for Assessing Adequacy of Treatment and Predicting Relapse in Patients Treated for Pulmonary Tuberculosis. Journal of Nuclear Medicine. 2020;**61**(3):412–417. DOI: 10.2967/jnumed.119.233783

[60] Rea G, Sperandeo M, Lieto R, Bocchino M, Quarato CMI, Feragalli B, Valente T, Scioscia G, Giuffreda E, Foschino Barbaro MP, Lacedonia D. Chest Imaging in the Diagnosis and Management of Pulmonary Tuberculosis: The Complementary Role of Thoracic Ultrasound. Frontiers in Medicine (Lausanne). 2021;**8**:753821. DOI: 10.3389/fmed.2021.753821

[61] Koo HK, Min J, Kim HW, Ko Y, Oh JY, Jeong YJ, Kang HH, Kang JY, Lee SS, Seo M, Silverman EK, Kim JS, Park JS. Cluster analysis categorizes five phenotypes of pulmonary tuberculosis. Scientific Reports. 2022;**12**(1):10084. DOI: 10.1038/s41598-022-13526-1

[62] Hrizi O, Gasmi K, Ben Ltaifa I, Alshammari H, Karamti H, Krichen M, Ben Ammar L, Mahmood MA. Tuberculosis Disease Diagnosis Based on an Optimized Machine Learning Model. Journal of Healthcare Engineering. 2022;**2022**:8950243. DOI: 10.1155/2022/8950243

[63] Ahamed Fayaz S, Babu L, Paridayal L, Vasantha M, Paramasivam P, Sundarakumar K, Ponnuraja C. Machine learning algorithms to predict treatment success for patients with pulmonary tuberculosis. PLoS One. 2024;**19**(10): e0309151. DOI: 10.1371/journal.pone.0309151

[64] Victor CN, Sreemoy KD. Evaluation of Queue Management System (QMS) Use in Chest X-Ray for Tuberculosis Screening: A Case Study. Indian Journal of Radiology and Imaging. 2025;**35**(4):558–567. DOI: 10.1055/s-0045-1805004

[65] Parreira PL, Fonseca AU, Soares F, Conte MB, Rabahi MF. Chest X-ray evaluation using machine learning to support the early diagnosis of pulmonary TB. International Journal of

Tuberculosis and Lung Disease. 2024;**28**(4):171–175. DOI: 10.5588/ijtld.23.0230

[66] Innes AL, Lebrun V, Hoang GL, Martinez A, Dinh N, Nguyen TTH, Huynh TP, Quach VL, Nguyen TB, Trieu VC. An effective health system approach to end TB: Implementing the double X strategy in Vietnam. Global Health: Science and Practice. 2024;12e2400024. DOI: 10.9745/GHSP-D-24-00024

[67] Ahamed Fayaz S, Babu L, Paridayal L, Vasantha M, Paramasivam P, Sundarakumar K, et al. Machine learning algorithms to predict treatment success for patients with pulmonary tuberculosis. PLoS ONE. 2024;**19**(10):e0309151. DOI: 10.1371/journal.pone.0309151

[68] Nijiati M, Zhou R, Damaola M, Hu C, Li L, Qian B, Abulizi A, Kaisaier A, Cai C, Li H, Zou X. Deep learning based CT images automatic analysis model for active/non-active pulmonary tuberculosis differential diagnosis. Frontiers in Molecular Biosciences. 2022;**9**(2022):1–5. DOI: 10.3389/fmolb.2022.1086047

[69] Maheswari BU, Sam D, Mittal N, Sharma A, Kaur S, Askar SS, Abouhawwash M. Explainable deep-neural-network supported scheme for tuberculosis detection from chest radiographs. BMC Medical Imaging. 2024;**24**(1):32. DOI: 10.1186/s12880-024-01202-x

[70] Shobayo O, Saatchi R. Developments in Deep Learning Artificial Neural Network Techniques for Medical Image Analysis and Interpretation. Diagnostics (Basel). 2025;**15**(9):1072. DOI: 10.3390/diagnostics15091072

[71] Annarumma M, Withey SJ, Bakewell RJ, Pesce E, Goh V, Montana G. Automated Triaging of Adult Chest Radiographs with Deep Artificial Neural Networks. Radiology. 2019;**291**(1):196–202. DOI: 10.1148/radiol.2018180921

[72] Sahar KBS, Atilla PK, Zaid NMS, Nsala S, Minyoi MBS, Brain SDM, et al. Prospective Multi-Site Validation of AI to Detect Tuberculosis and Chest X-Ray Abnormalities. NEJM AI. 2024;**1**(10):1–5. DOI: 10.1056/AIoa2400018

[73] Vinayak S, Nillmani, Sachin KG, Kaushal KS. Deep learning models for tuberculosis detection and infected region visualization in chest X-ray images. Intelligent Medicine. 2024;**4**(2):104–113. DOI: 10.1016/j.imed.2023.06.001

[74] Qin ZZ, Sander MS, Rai B, Titahong CN, Sudrungrot S, Laah SN, Adhikari LM, et al Using artificial intelligence to read chest radiographs for tuberculosis detection: A multi-site evaluation of the diagnostic accuracy of three deep learning systems. Scientific Reports. 2019;**9**:15000

[75] Paras L, Baskaran S.Deep learning at chest radiography: Automated classification of pulmonary tuberculosis by using convolutional neural networks. Radiology. 2017;**284**(2). DOI: 10.1148/radiol.2017162326

[76] Zhang X, Dong X, Saripan MIB, Du D, Wu Y, Wang Z, Cao Z, Wen D, Liu Y, Marhaban MH. Deep learning PET/CT-based radiomics integrates clinical data: A feasibility study to distinguish between tuberculosis nodules and lung cancer. Thoracic Cancer. 2023;**14**(19):1802–1811. DOI: 10.1111/1759-7714.14924

[77] Wu S, Wang X, Ji J, Geng G, Zhang Z, Hou D. A preliminary investigation on a deep learning convolutional neural networks based pulmonary tuberculosis CT diagnostic model (in Chinese). Chinese Journal of Tuberculosis and Respiratory Diseases. 2021;**44**:450–455. DOI: 10.3760/cma.j.cn112147-20210108-00026

[78] Yan C, Lin J, Li H, Xu J, Zhang T, Chen H, Woodruff HC, Wu G, Zhang S, Xu Y, Lambin P. Cycle-Consistent Generative Adversarial Network: Effect on Radiation Dose Reduction and Image Quality Improvement in Ultralow-Dose CT for Evaluation of Pulmonary Tuberculosis. Korean Journal of Radiology. 2021;**22**(6):983–993. DOI: 10.3348/kjr.2020.0988

[79] Zhang Y, Liu M, Zhang L, et al. Comparison of Chest Radiograph Captions Based on Natural Language Processing vs Completed by Radiologists. JAMA Network Open. 2023;**6**(2):e2255113. DOI: 10.1001/jamanetworkopen.2022.55113

[80] Iftikhar S, Naz I, Zahra A, Zaidi SY. Report Generation of Lungs Diseases from Chest X-ray using NLP. International Journal of Innovations in Science & Technology. 2022;**3**(4):223–233

[81] Velo A, Chen SX, Adler S, Ayoub N, Lim S, Wang HY, et al. Diagnosis of an active tuberculosis infection utilizing natural language processing. Chest. 2024;**166**(4): A1568–A1569. DOI: 10.1016/j.chest.2024.06.994

[82] Zulkifli Z, Retno AS, Sfenrianto S, Zulvi W, Panji B, et al. Expert System for Diagnosis of Lung Disease from X-Ray Using CNN and SVM. International Journal of Artificial Intelligence Research. 2023;7(2):1–5. DOI: 10.29099/ijair.v7i1.870

[83] Yablonskii P, Kudriashov G, Vasilev I, Avetisyan A, Sokolova O. Robot-assisted surgery in complex treatment of the pulmonary tuberculosis. Journal of Visualized Surgery. 2017;**3**:18. DOI: 10.21037/jovs.2016.12.09

[84] Yablonskii P, Kudriashov G, Kiryukhina L, Avetisyan A. Robot-assisted thoracoscopic right upper bi-lobectomy for pulmonary tuberculosis. Journal of Visualized Surgery. 2018;**4**:48. DOI: 10.21037/jovs.2018.03.03

[85] Kukker A, Sharma R, Pandey G, Faseehuddin M. Fuzzy lattices assisted EJAYA Q-learning for automated pulmonary diseases classification. Biomedical Physics & Engineering Express. 2024;**10**(6). DOI: 10.1088/2057-1976/ad72f8